1362 (1955).
[13]J. C. Slater, *Quantum Theory of Atomic Structure* (McGraw-Hill, New York, 1960), Vols. I and II.
[14]D. C. Reynolds, C. W. Litton, and T. C. Collins, Phys. Status Solidi 9, 645 (1965); 12, 3 (1965).
[15]D. W. Langer *et al.* (unpublished). I thank Dr. Langer for communicating his results to me before publication.

PHYSICAL REVIEW B VOLUME 3, NUMBER 2 15 JANUARY 1971

Energy Levels of Direct Excitons in Semiconductors with Degenerate Bands*

A. Baldereschi and Nunzio C. Lipari
Department of Physics and Materials Research Laboratory, University of Illinois, Urbana, Illinois 62802
(Received 2 September 1970)

A new method to investigate the direct-exciton spectrum in semiconductors with degenerate bands is described. This method, which solves the effective-mass Hamiltonian using symmetry arguments and second-order perturbation theory, gives a general and accurate description of exciton states in semiconductors. Direct excitons in group-IV elements, III-V compounds, and II-VI compounds are investigated. For Ge and GaAs, the binding energy is in excellent agreement with previous calculations. For all other substances, our treatment represents the first theoretical investigation. The results are in satisfactory agreement with available experimental data.

I. INTRODUCTION

Diamond and zinc-blende semiconductors have been studied extensively in recent years and a large amount of information is now available both experimentally and theoretically. Special attention has been given to the optical properties because they are one of the best tools for investigating band structures and electron states. Near the fundamental edge, the optical spectra of these semiconductors exhibit structure which is interpreted as due to direct-exciton formation. In large-gap semiconductors, additional structure due to indirect excitations is observed at lower energies.

The first observation of direct and indirect excitons was made in Si and Ge.[1] Since then, structure due to exciton formation has been observed in many zinc-blende III-V[2] and II-VI[3] compounds. These effects are generally small, owing to the large dielectric constants and small effective masses of these materials. For InSb, these effects are so small that they have not yet been observed in optical spectra. In this case, however, exciton effects have been observed in magneto-optical experiments[4] and the exciton binding energy can be estimated.

In contrast to such abundance of experimental data, little theoretical work has been done up to date. Most of these theoretical investigations have been concerned with the exciton energy spectrum and the optical absorption in a model semiconductor with simple valence and conduction bands. In this case, the Wannier exciton Hamiltonian[5] can be reduced to that of the hydrogen atom and exact solutions are easily obtained. Optical selection rules and the absorption coefficient have been investigated[6] in detail too. Even though these investigations are useful from the theoretical point of view, they cannot be applied directly to the interpretation of most of the experimental data because degeneracies often occur in the energy bands. All crystals with the diamond and zinc-blende structure have a degenerate valence band at $\vec{k} = 0$, where the exciton is formed, and therefore the theory for simple bands cannot be applied.

A formal theoretical treatment of excitons in the case of degenerate bands has been done by Dresselhaus.[7] The resulting Hamiltonian is formally similar to that describing impurity states for degenerate bands[8] and, owing to its complexity, no exact solutions have been obtained. McLean and Loudon[9] have obtained an approximate solution for the ground state of the direct and the indirect excitons in Ge and Si using the variational technique previously introduced by Kohn and Schechter[10] in their treatment of shallow acceptor states. The same method was also used by Abe,[11] who considered the direct exciton in Ge and GaAs. So far, no one has considered the exciton series originating from the split-off valence band whose effects in optical spectra have been experimentally observed.[12–14] Furthermore, no calculations have been done to compute the energy of excited states which have been experimentally observed in some of the III-V compounds[15] and II-VI compounds.[16] The reason for these facts is that the variational technique, which involves elaborate computations for the ground state, becomes practically impossible when applied to excited states or to the split-off exciton series.

To avoid the above computational difficulties the exciton spectra in these cases have been roughly estimated using a model in which the degenerate valence band is replaced by an "average" simple band. Owing to the complexity of the valence band, this model is expected to be poor. Valence-band parameters are now available for crystals with the diamond and zinc-blende lattices.[17] It would be therefore desirable to obtain exciton energy spectra which take into account the details of the valence band.

In a previous paper[18] we have outlined a simple method based on the symmetry properties of the exciton effective-mass Hamiltonian and second-order perturbation theory, which can be applied to an arbitrary number of bands and to any lattice. We have given there a simple analytical expression for the binding energy of direct excitons in diamond and zinc-blende crystals neglecting effects from the split-off band.

The purpose of the present paper is to describe in detail this method and to give a general investigation of the direct-exciton spectra in diamond and zinc-blende crystals. Analytical expressions for the binding energy of the ground state and the first excited state are obtained for both the main and the split-off exciton series. The intrinsic lifetime of the split-off exciton states is calculated too.

In Sec. II we give the general formulation of the problem and the method of solution. In Sec. III we apply the method to diamond and zinc-blende crystals. The results are compared with available experimental data and discussed. In Sec. IV we summarize the main results of the present investigation and discuss possible extensions of the method.

II. FORMULATION OF PROBLEM AND METHOD OF SOLUTION

The band structure of crystals with the diamond and zinc-blende lattice have been studied extensively[19] and are very similar. The direct gap is at $\vec{k}=0$, where the conduction band has a nondegenerate minimum and the valence band has a threefold-degenerate maximum, neglecting spin. The inclusion of spin and spin-orbit interaction alters the bands by splitting the sixfold-degenerate valence states into an upper fourfold ($J=\frac{3}{2}$) state and a lower twofold ($J=\frac{1}{2}$) state separated by a spin-orbit splitting Δ. The structure of the valence and conduction bands in the vicinity of $\vec{k}=0$ is shown in Fig. 1(a), where the states are labeled by the irreducible representation to which they belong. The absence of inversion symmetry for zinc-blende crystals leads to the presence of very small linear terms in $\vec{k}$[20] in the energy-versus-momentum expression. These terms, which are generally very small and only rarely lead to observable effects,[21] slightly displace the valence-band maximum from $\vec{k}=0$.

Figure 1(a) shows that, in diamond and zinc-blende crystals, two different direct-exciton series can be formed. The first (which will be called main series hereafter) is fourfold degenerate and originates from the upper valence band; the second (split-off series) is twofold degenerate and originates from the lower valence band. The two series are displaced by the spin-orbit splitting Δ and are schematically shown in Fig. 1(b). For the kind of band structure represented in Fig. 1(a), the Hamiltonian for the relative electron-hole motion is (neglecting the electronic spin)[8]

$$H_{ex}(\vec{p})=\left(\frac{p^2}{2m_e^*}-\frac{e^2}{\epsilon r}\right)I-H_v(\vec{p}), \tag{1}$$

where $\vec{p}$ is the relative electron-hole momentum, m_e^* is the electron effective mass, ϵ is the static dielectric constant, r is the electron-hole distance, I is the 6×6 unit matrix, and H_v is the well-known 6×6 matrix[22] which describes the hole kinetic energy near $\vec{k}=0$. Equation (1) differs for diamond and zinc-blende structures because of linear terms in $\vec{p}$ which appear in H_v in the latter case. We shall therefore treat separately the two lattices.

A. Crystals with Diamond Structure

We first consider the diamond case and write Eq. (1) in matrix form as follows:

$$H_{ex}(\vec{p})=\begin{vmatrix} P+Q & L & +M & 0 & (i/\sqrt{2})L & -i\sqrt{2}M \\ L^* & P-Q & 0 & M & -i\sqrt{2}Q & i(\sqrt{\tfrac{3}{2}})L \\ M^* & 0 & P-Q & -L & -i(\sqrt{\tfrac{3}{2}})L^* & -i\sqrt{2}Q \\ 0 & M^* & -L^* & P+Q & -i\sqrt{2}M^* & -(i/\sqrt{2})L^* \\ (-i/\sqrt{2})L^* & i\sqrt{2}Q & i(\sqrt{\tfrac{3}{2}})L & i\sqrt{2}M & P+\Delta & 0 \\ i\sqrt{2}M^* & -i(\sqrt{\tfrac{3}{2}})L^* & i\sqrt{2}Q & (i/\sqrt{2})L & 0 & P+\Delta \end{vmatrix}, \tag{2}$$

where

$$P=\frac{p^2}{2\mu_0}-\frac{e^2}{\epsilon r} \quad (s\text{-like}), \tag{3a}$$

$$Q=\frac{p_x^2+p_y^2-2p_z^2}{2\mu_1} \quad (d\text{-like}), \tag{3b}$$

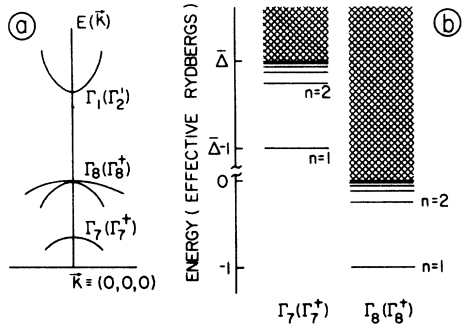

FIG. 1. (a) Schematic plot of the conduction and valence bands for diamond and zinc-blende crystals near $\vec{k}=0$. Their irreducible representations are also indicated. (b) Energy levels of the two direct-exciton series originating from the band structure shown in (a).

$$L=-i\frac{(p_x-ip_y)p_z}{2\mu_2} \qquad (d\text{-like}), \tag{3c}$$

$$M=+\sqrt{3}\frac{p_x^2-p_y^2}{2\mu_1}-i\frac{p_xp_y}{2\mu_2} \qquad (d\text{-like}). \tag{3d}$$

In the above expressions we have introduced the masses μ_0, μ_1, and μ_2 which are the most natural choices for the description of the valence and conduction bands in the exciton Hamiltonian. They are related to the Luttinger parameters[23] γ_1, γ_2, and γ_3 and to the Dresselhaus-Kip-Kittel parameters[24] A, B, and C as follows:

$$\frac{1}{\mu_0}=\frac{1}{m_e^*}+\frac{\gamma_1}{m_0}=\frac{1}{m_e^*}-\frac{2}{\hbar^2}A, \tag{4a}$$

$$\frac{1}{\mu_1}=\frac{\gamma_2}{m_0}=-\frac{1}{\hbar^2}B, \tag{4b}$$

$$\frac{1}{\mu_2}=2\sqrt{3}\frac{\gamma_3}{m_0}=\frac{2}{\hbar^2}(C^2+3B^2)^{1/2}, \tag{4c}$$

where m_0 is the free-electron mass. Under the operations of the rotation group, the operators (3a)–(3d) have different symmetry properties, which are indicated to the right. In accordance with this, it is natural to write (2) as follows:

$$H_{ex}=H_s+H_d, \tag{5}$$

where H_s and H_d are 6×6 matrices which contain only s-like and d-like, operators, respectively. Their explicit expressions are

$$H_s=\begin{vmatrix} P & 0 & 0 & 0 & 0 & 0 \\ 0 & P & 0 & 0 & 0 & 0 \\ 0 & 0 & P & 0 & 0 & 0 \\ 0 & 0 & 0 & P & 0 & 0 \\ 0 & 0 & 0 & 0 & P+\Delta & 0 \\ 0 & 0 & 0 & 0 & 0 & P+\Delta \end{vmatrix}, \tag{6a}$$

and

$$H_d=\begin{vmatrix} Q & L^* & M & 0 & (i/\sqrt{2})L & -i\sqrt{2}M \\ L^* & -Q & 0 & M & -i\sqrt{2}Q & i(\sqrt{\tfrac{3}{2}})L \\ M^* & 0 & -Q & -L & -i(\sqrt{\tfrac{3}{2}})L^* & -i\sqrt{2}Q \\ 0 & M^* & -L^* & Q & -i\sqrt{2}M^* & (-i/\sqrt{2})L^* \\ (-i/\sqrt{2})L^* & i\sqrt{2}Q & i(\sqrt{\tfrac{3}{2}})L & i\sqrt{2}M & 0 & 0 \\ i\sqrt{2}M^* & -i(\sqrt{\tfrac{3}{2}})L^* & i\sqrt{2}Q & (i/\sqrt{2})L & 0 & 0 \end{vmatrix}. \tag{6b}$$

The operators (6a) and (6b) have a simple physical meaning. The former represents an exciton which results from the Coulomb interaction between the electron and the isotropic part of the hole; the latter describes the anisotropy in the valence band.

From expressions (4a)–(4c), the masses μ_1 and μ_2 are expected to be much larger than μ_0 because the electron effective mass appears only in the latter. For this reason the operators (3b)–(3d) should be much smaller than (3a), so the H_d in (5) can be considered as a perturbation with respect to H_s. The validity of this assumption has been verified for a few substances in our previous paper[18] and will be confirmed for all crystals with the diamond and zinc-blende structure from the results which are presented in Sec. II B.

We first analyze eigenstates and eigenvalues of the unperturbed Hamiltonian H_s. Exact solutions of this Hamiltonian are easily found because the operator P represents the Hamiltonian of a hydrogen atom with reduced mass μ_0 and dielectric constant ϵ. The eigenstates of (6a) consist of six exciton spectra which can be grouped into two different series, fourfold and twofold degenerate, respectively, separated by the spin-orbit splitting Δ. These two series, which are represented in Fig. 1(b), have the same effective Rydberg

$$R_0=\mu_0e^4/2\hbar^2\epsilon^2, \tag{7}$$

and the same effective Bohr radius

$$a_0=\epsilon\hbar^2/\mu_0e^2. \tag{8}$$

From now on, we use expressions (7) and (8) as units of energy and length, respectively.

The eigenfunctions of the discrete spectrum can be classified with the quantum numbers n, l, m, and i, where the first three are the usual hydrogen-atom quantum numbers and $i = 1, 2, \ldots, 6$ denotes the various exciton series. For the continuum, the quantum number n is to be replaced by the continuous variable k. The wave functions can be written as

$$\left|\begin{bmatrix} n \\ k \end{bmatrix}, l, m, i\right\rangle = \left|\begin{bmatrix} n \\ k \end{bmatrix}, l, m\right\rangle \cdot |i\rangle , \tag{9}$$

where

$$\left|\begin{bmatrix} n \\ k \end{bmatrix}, l, m\right\rangle$$

are the usual hydrogen-atom wave functions as given given, e.g., in Ref. 25, and $|i\rangle$ are the spinors

$$|i\rangle = \begin{pmatrix} \delta_{1i} \\ \delta_{2i} \\ \delta_{3i} \\ \delta_{4i} \\ \delta_{5i} \\ \delta_{6i} \end{pmatrix} , \tag{10}$$

where δ_{ij} is the Kronecker function. The corresponding eigenvalues for the discrete spectra are

$$E_{n,i} = \begin{cases} -1/n^2 , & i = 1, 2, 3, 4 \\ \bar{\Delta} - 1/n^2 , & i = 5, 6 \end{cases} \tag{11}$$

where $\bar{\Delta}$ is the spin-orbit splitting Δ measured in units of the effective Rydberg. For the continuum, the energies are still given by (11) with the replacement $n = -i/k$.

We now consider the operator H_d and limit ourselves to the lowest two bound states in each series (the $1s$ and $2s$ exciton states) because so far these are the only states for which experimental evidence is available. It is easily seen that, for these states, the first nonvanishing contribution comes from second-order degenerate perturbation theory. The resulting secular determinant is diagonal and therefore nondegenerate perturbation theory can be used. For the $1s$ and $2s$ states of the main series the H_d contribution is

$$\Delta E_d(1s) = \sum_{i=1}^{6} \left\{ \sum_{n,l,m} \frac{|\langle n,l,m,i \mid H_d \mid 1,0,0,1\rangle|^2}{-1 - E_{n,i}} + \sum_{l,m} \int_0^\infty dk \, \frac{|\langle k,l,m,i \mid H_d \mid 1,0,0,1\rangle|^2}{-1 - E_{k,i}} \right\} \tag{12a}$$

and

$$\Delta E_d(2s) = \sum_{i=1}^{6} \left\{ \sum_{n,l,m} \frac{|\langle n,l,m,i \mid H_d \mid 2,0,0,1\rangle|^2}{-\frac{1}{4} - E_{n,i}} + \sum_{l,m} \int_0^\infty dk \, \frac{|\langle k,l,m,i \mid H_d \mid 2,0,0,1\rangle|^2}{-\frac{1}{4} - E_{k,i}} \right\} , \tag{12b}$$

and, for the same states of the split-off series, is

$$\Delta E_d^{so}(1s) = \sum_{i=1}^{4} \left\{ \sum_{n,l,m} \frac{|\langle n,l,m,i \mid H_d \mid 1,0,0,5\rangle|^2}{\bar{\Delta} - 1 - E_{n,i}} + \sum_{l,m} \int_0^\infty dk \, \frac{|\langle k,l,m,i \mid H_d \mid 1,0,0,5\rangle|^2}{\bar{\Delta} - 1 - E_{k,i}} \right\} , \tag{12c}$$

$$\Delta E_d^{so}(2s) = \sum_{i=1}^{4} \left\{ \sum_{n,l,m} \frac{|\langle n,l,m,i \mid H_d \mid 2,0,0,5\rangle|^2}{\bar{\Delta} - \frac{1}{4} - E_{n,i}} + \sum_{l,m} \int_0^\infty dk \, \frac{|\langle k,l,m,i \mid H_d \mid 2,0,0,5\rangle|^2}{\bar{\Delta} - \frac{1}{4} - E_{k,i}} \right\} . \tag{12d}$$

In the above expressions, the summations on n, l, and m extend over all possible values excluding the initial state.

In the Appendix we consider expressions (12a)–(12d) and we show that they can be written as follows:

$$\Delta E_d(1s) = -\tfrac{4}{5} \Phi(\mu_0, \mu_1, \mu_2) \left[S_1(0) + S_1(\bar{\Delta}) \right] , \tag{13a}$$

$$\Delta E_d(2s) = -\tfrac{1}{10} \Phi(\mu_0, \mu_1, \mu_2) \left[S_2(0) + S_2(\bar{\Delta}) \right] , \tag{13b}$$

$$\Delta E_d^{so}(1s) = -\tfrac{8}{5} \Phi(\mu_0, \mu_1, \mu_2) \, T_1(\bar{\Delta}) , \tag{13c}$$

$$\Delta E_d^{so}(2s) = -\tfrac{1}{5} \Phi(\mu_0, \mu_1, \mu_2) \, T_2(\bar{\Delta}) , \tag{13d}$$

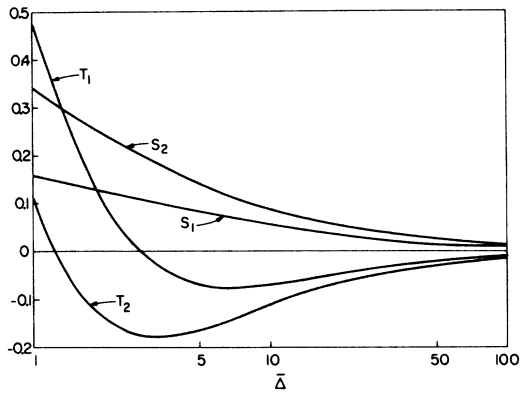

FIG. 2. Plot of the functions S_1, S_2, T_1, and T_2 versus the spin-orbit splitting $\bar{\Delta}$, which is in units of the effective Rydberg.

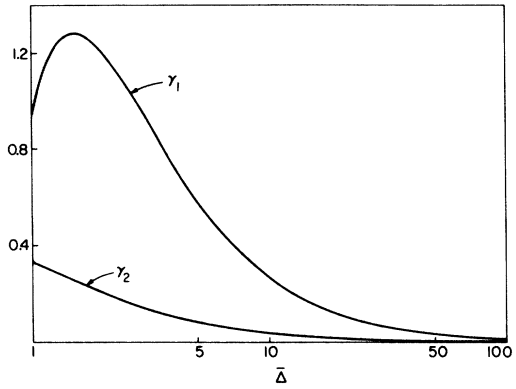

FIG. 3. Values of γ_1 and γ_2 as functions of the spin-orbit splitting $\bar{\Delta}$, which is in units of the effective Rydberg.

where the functions S_1, S_2, T_1, and T_2 are defined in the Appendix and are shown in Fig. 2 for $\bar{\Delta} \geq 1$. Some numerical values are given in Table I. In expressions (13a)–(13d) we have introduced the parameter

$$\Phi(\mu_0, \mu_1, \mu_2) = 8\,(\mu_0/\mu_1)^2 + (\mu_0/\mu_2)^2\,, \qquad (14)$$

which depends only on the electron and hole effective masses and gives the strength of the interactions described by the operator H_d. These interactions are of two different kinds: the "intraseries" interaction between levels of the main series and the "interseries" interaction between levels belonging to different series. Note that the coupling strength Φ is the same for the two kinds of interactions and that the operator H_d does not couple levels of the split-off series.

The unperturbed energy (11) together with the corrections (13a)–(13b) describes the low-energy bound states of the main series. Expression (11) together with (13c)–(13d) describes the low-energy spectrum of the split-off series. These latter states are degenerate with the continuum of the main series as shown in Fig. 1(b) and interact with it through H_d, so that, besides being shifted by the energies (13c)–(13d), they are broadened.

The half-width of these states can be computed with the method of Ref. 26 and is given by

$$\Gamma_{1s}^{so} = \pi \sum_{i=1}^{4} \sum_{l,m} |\langle k, l, m, i \,|\, H_d \,|\, 1, 0, 0, 5\rangle|^2\,, \qquad (15a)$$

$$\Gamma_{2s}^{so} = \pi \sum_{i=1}^{4} \sum_{l,m} |\langle k, l, m, i \,|\, H_d \,|\, 2, 0, 0, 5\rangle|^2\,, \qquad (15b)$$

where k is such that the two states in the above matrix elements have the same energy. As shown in the Appendix, expressions (15a) and (15b) can be written as

$$\Gamma_{1s}^{so} = \Phi(\mu_0, \mu_1, \mu_2)\,\gamma_1(\bar{\Delta}), \qquad (16a)$$

$$\Gamma_{2s}^{so} = \Phi(\mu_0, \mu_1, \mu_2)\,\gamma_2(\bar{\Delta}), \qquad (16b)$$

with the functions γ_1 and γ_2 defined there. These functions are shown in Fig. 3 for $\bar{\Delta} \geq 1$ and some numerical values are given in Table I.

TABLE I. Numerical values of the functions S_1, S_2, T_1, T_2, γ_1, and γ_2 defined in the text.

$\bar{\Delta}$	S_1	S_2	T_1	T_2	γ_1	γ_2
0	0.2246	0.7029	. . .	. . .	. . .	. . .
1	0.1587	0.3420	0.4751	0.1119	0.9235	0.3350
2	0.1268	0.2452	0.0983	−0.1421	1.2018	0.2067
3	0.1070	0.1953	−0.0161	−0.1767	0.9310	0.1411
4	0.0932	0.1638	−0.0555	−0.1737	0.7248	0.1042
5	0.0830	0.1419	−0.0699	−0.1627	0.5810	0.0812
6	0.0750	0.1257	−0.0745	−0.1504	0.4785	0.0656
8	0.0633	0.1029	−0.0733	−0.1287	0.3452	0.0463
10	0.0550	0.0875	−0.0672	−0.1106	0.2643	0.0350
20	0.0341	0.0514	−0.0456	−0.0661	0.1090	0.0140
50	0.0168	0.0240	−0.0218	−0.0296	0.0311	0.0038
100	0.0094	0.0130	−0.0116	−0.0154	0.0116	0.0015

B. Crystals with Zinc-Blende Structure

In this case, the exciton Hamiltonian is equal to that of the diamond case, expression (2), plus a 6×6 matrix whose elements are linear in $\vec{p}$ and which expresses inversion-asymmetry effects

$$H_{ex}^{zb} = H_{ex}^{diam} + H_p = H_s + H_d + H_p . \tag{17}$$

As already said, the contribution from the last term in (17) is generally extremely small. In order to establish the magnitude of this contribution, we now consider the inversion-asymmetry effect on the ground state of the main series, neglecting the interaction with the split-off series, this being even smaller. Under this assumption, $H_p(\vec{p})$ is the following 4×4 matrix[20]:

$$H_p(\vec{p}) = \begin{vmatrix} 0 & U & -V & \sqrt{3}\,U^+ \\ U^+ & 0 & -\sqrt{3}\,U & V \\ -V & -\sqrt{3}\,U^+ & 0 & U \\ \sqrt{3}\,U & V & U^+ & 0 \end{vmatrix} , \tag{18}$$

where

$$U = \tfrac{1}{2}\sqrt{3}\,\frac{\mu_0}{\mu_3}\left(\frac{\partial}{\partial x} + i\,\frac{\partial}{\partial y}\right) \quad (p\text{-like}), \tag{19a}$$

$$V = i\sqrt{3}\,\frac{\mu_0}{\mu_3}\,\frac{\partial}{\partial z} \quad (p\text{-like}), \tag{19b}$$

and the units (7) and (8) have been used. In expressions (19a) and (19b) we have introduced the inversion-asymmetry effective mass μ_3, which is related to the previously used parameter[27] C as follows:

$$\mu_3 = \tfrac{1}{2}\sqrt{3}\,(\hbar^2/a_0)\,(1/C) . \tag{20}$$

We now solve Hamiltonian (17) following exactly the same technique used in the case of (5). In this case the perturbation term is $H_d + H_p$. The contribution from H_d is given by expression (13a) and therefore we have to consider only the effect of (18). In this case too, the first nonvanishing contribution to the ground-state energy comes from second-order degenerate perturbation theory and is

$$\Delta E_p(1s) = \sum_{i=1}^{4}\left\{\sum_{n,l,m}\frac{|\langle n,l,m,i\,|\,H_p\,|\,1,0,0,1\rangle|^2}{-1-E_{n,i}} + \sum_{l,m}\int_0^\infty dk\,\frac{|\langle k,l,m,i\,|\,H_p\,|\,1,0,0,1\rangle|^2}{-1-E_{k,i}}\right\} . \tag{21}$$

As shown in the Appendix, expression (21) can be written as

$$\Delta E_p(1s) = -12\,(\mu_0/\mu_3)^2\,S_3(0) = -\tfrac{9}{4}\,(\mu_0/\mu_3)^2 \tag{22}$$

in units of the effective Rydberg. The quantity $S_3(0)$ is defined in the Appendix, where its value $S_3(0) = \frac{3}{16}$ is derived. Since the inversion-asymmetry mass μ_3 is infinite for the diamond case and generally extremely large for the zinc-blende case, we obtain that the contribution (22) is vanishing in the former case, as it has to be, and very small in the latter.

Before applying our method to actual cases, we summarize the results of this section. We have separated the total exciton Hamiltonian into two parts. The first one (H_s) describes the main and split-off exciton spectra as being perfectly hydrogenic and noninteracting. The second part (H_d or $H_d + H_p$ for diamond or zinc-blende lattices, respectively) introduces the interseries and intraseries couplings. This second part destroys the Rydberg law in both series and its contribution to the energy levels has been treated by perturbation theory. Our results show that the strength of both interactions depends on the coupling parameter Φ and that the relative magnitude of the interseries and intraseries interactions is a function of the parameter $\bar{\Delta}$. Figure 2 shows that the larger the $\bar{\Delta}$, the smaller the ratio between interseries and intraseries interactions.

III. RESULTS AND DISCUSSION

Our purpose is threefold: (i) Test the validity of the perturbation treatment; (ii) compare its accuracy with respect to the variational approach; and (iii) apply our method to investigate the main and split-off exciton series in all crystals with the diamond and zinc-blende structure for which band parameters are available.

Table II gives the parameters used in the calculation together with the energy gap E_g and an estimate of the binding energy E_b of the exciton main series obtained assuming an infinite mass for the hole. For every substance shown, we give various sets of valence-band parameters as obtained theoretically or experimentally by different authors. From the values shown in Table II we can test the validity of our treatment. The requirements $\mu_0/\mu_1 < 1$ and $\mu_0/\mu_2 < 1$ are always verified, so that the parameter Φ, which is a measure of the strength of the perturbation, is always small and therefore our treatment is valid.

Furthermore, in going from Hamiltonian (1) to its explicit expression (2), we have implicitly accepted the assumption that the upper and lower valence bands have the same isotropic mass. This assumption is valid only when $\Delta/E_g \ll 1$, a condition which is generally, but not always, satisfied for the substances shown in Table II. For GaSb, InAs, and InSb the above condition is not verified and, in effect, a difference in the valence-band masses has been actually experimentally observed in InAs[14]

TABLE II. Parameters used in the calculations. Static dielectric constant ϵ_0, electron effective mass m_e^*, exciton reduced masses μ_0, μ_1, and μ_2 defined in the text, spin-orbit splitting Δ, and energy gap E_g. The value of the coupling parameter Φ and an estimate of the exciton binding energy E_b are also given. The upper indices refer to references. The energy unit is meV.

	ϵ_0	m_e^*/m_0	μ_0/m_0	μ_1/m_0	μ_2/m_0	E_g	Δ	E_b	Φ
AlSb	9.9 [28]	0.011 [50]	0.010 [17]	1.835 [17]	0.202 [17]	2220 [51, 52]	750 [38]	1.5	0.003 [17]
			0.010 [43]	0.500 [43]	0.153 [43]				0.008 [43]
GaP	11.1 [29]	0.13 [50]	0.075 [17]	−18.182 [17]	0.271 [17]	2740 [52, 53]	90 [53, 59]	14.4	0.077 [17]
			0.081 [43]	0.769 [43]	0.185 [43]				0.279 [43]
GaAs	12.5 [30]	0.066 [37]	0.048 [17]	0.823 [17]	0.148 [17]	1520 [16]	340 [52, 58]	5.7	0.130 [17]
			0.048 [43]	0.444 [43]	0.129 [43]				0.235 [43]
			0.045 [63]	0.400 [60]	0.115 [60]				0.250 [60]
GaSb	15.2 [31]	0.047 [50,38]	0.035 [17]	0.444 [17]	0.100 [17]	810 [54]	800 [52, 57]	2.8	0.169 [17]
			0.032 [43]	0.233 [43]	0.065 [43]				0.389 [43]
			0.031 [47]	0.333 [47]	0.066 [47]				0.289 [47]
InP	12.1 [32]	0.077 [39]	0.053 [17]	0.719 [17]	0.141 [17]	1310 [39, 52]	240 [39]	7.2	0.188 [17]
			0.052 [43]	0.377 [43]	0.109 [43]				0.378 [43]
InAs	11.8 [33]	0.024 [39,40]	0.018 [17]	0.157 [17]	0.042 [17]	410 [39, 55]	380 [14]	2.3	0.280 [17]
			0.017 [43]	0.131 [43]	0.038 [43]				0.345 [43]
			0.016 [40]	0.111 [40]	0.032 [40]				0.419 [40]
InSb	16.8 [31]	0.015 [41]	0.012 [17]	0.117 [17]	0.032 [17]	240 [5]	810 [14, 52]	0.7	0.213 [17]
			0.010 [43]	0.068 [43]	0.019 [43]				0.457 [43]
			0.010 [48]	0.069 [48]	0.018 [48]				0.460 [48]
Ge	15.4 [34]	0.038 [42]	0.026 [43]	0.250 [43]	0.059 [43]	890 [56]	290 [13]	2.2	0.282 [43]
			0.025 [49]	0.233 [49]	0.051 [49]				0.340 [49]
ZnS	8.1 [35]	0.39 [43]	0.178 [17]	−3.774 [17]	0.575 [17]	3800 [57]	72 [4]	80.9	0.113 [17]
			0.229 [43]	1.036 [43]	0.381 [43]				0.749 [43]
ZnSe	8.7 [36]	0.17 [44]	0.125 [17]	4.167 [17]	0.423 [17]	2800 [50, 4]	430 [4]	30.6	0.094 [17]
			0.132 [43]	0.837 [43]	0.215 [43]				0.573 [43]
ZTe	10.1 [35]	0.09 [45]	0.069 [17]	25.000 [17]	0.389 [17]	2390 [45, 4]	900 [4]	12.0	0.032 [17]
			0.081 [43]	0.840 [43]	0.244 [43]				0.186 [43]
CdTe	9.7 [35]	0.096 [46]	0.079 [17]	1.942 [17]	0.327 [17]	1610 [4]	900 [4]	13.9	0.072 [17]
			0.070 [43]	0.500 [43]	0.172 [43]				0.322 [43]

and GaSb.[12] For these substances Eq. (2) is still valid as long as one changes the reduced effective mass of the split-off series. This change does not affect in any way our treatment. All that has to be done is to introduce a different effective Rydberg for the split-off exciton. In fact, the interseries coupling, which should have been reconsidered because the two series have two different Bohr radii, can be neglected due to the fact that, in these semiconductors, $\bar{\Delta} > 100$, as shown in Table II.

We now consider the accuracy of our method with respect to the variational approach. The perturbation treatment is expected to have the same, or even higher, accuracy than the variational approach as long as the coupling parameter Φ is sufficiently weak. Variational calculations have been performed by Abe[11] for the binding energy of the main exciton in Ge and GaAs, assuming an infinite spin-orbit splitting Δ for both substances and neglecting the inversion-asymmetry effect for GaAs. The values of the parameters used by Abe are $\epsilon_0 = 16.0$, $\mu_0 = 0.025$, $\mu_1 = 0.224$, and $\mu_2 = 0.051$ for Ge, and $\epsilon_0 = 12.9$, $\mu_0 = 0.049$, $\mu_1 = 0.652$, and $\mu_2 = 0.095$ for GaAs. His results for the binding energy are 1.40 and 4.22 meV for Ge and GaAs, respectively. Using expressions (11) and (13a) (with $\bar{\Delta} = \infty$) together with (7), we obtain exactly the same results for both substances. Another variational calculation for the direct exciton in Ge has been done by McLean and Loudon[9] using the parameters $\epsilon_0 = 16.0$, $\mu_0 = 0.025$, $\mu_1 = 0.225$, and $\mu_2 = 0.054$, and they obtain a binding energy of 1.38 meV. Using the same parameters we obtain a value of 1.39 meV, which is in very good agreement. We note, looking at Table II, that Ge has one of the highest values of the coupling parameter Φ and therefore, since in this case the accuracy of our method is as good as that of the variational treatment, we conclude that, for all the other substances, our method will be even more accurate.

Having established the accuracy of our method, we now apply it to an investigation of the main and

split-off direct-exciton spectra in Ge III-V and II-VI compounds using the parameters given in Table II. In this table the inversion-asymmetry effective mass μ_3 is not given because such mass has not been evaluated so far and, to our knowledge, its value is known only for InSb, where Pidgeon and Groves[48] estimate $\mu_3 = 0.872 m_0$. Assuming this value, and using Eq. (22) together with (7), we find that linear terms in $\vec{p}$ contribute 0.0005 meV to the binding energy of the main exciton in InSb, which in Table II is roughly estimated 0.7 meV. Even considering a large uncertainty for the value of μ_3 given above, it is clear that this contribution is extremely small. For other substances, since the value of μ_3 is not known, we cannot evaluate the inversion-asymmetry contribution. The previous result for InSb, together with the fact that effects from linear terms are very difficult to be observed in all substances, guarantees that the results that we are going to give will not be affected by the inversion-asymmetry effect.

In Tables III and IV we give the results of our investigation for the III-V and II-VI compounds, respectively. In Table III we have also included Ge. In these tables we give the binding energies $E_b(1s, \Gamma_8)$ and $E_b(1s, \Gamma_6)$ of the ground state for the main and split-off series, respectively. Also included is the binding energy $E_b(2s, \Gamma_8)$ of the first excited state of the main series. These binding energies have been obtained using expressions (11) and (13a)–(13d) together with (7). The different contributions to the binding energy $E_b(1s, \Gamma_8)$ are also explicitly given. R_0 represents the H_s contribution; E_d and E_{so} represent the contribution from intraseries and interseries interactions, respectively.

We can see that E_d and E_{so} are much smaller than R_0, so that the condition of applicability of perturbation theory is well verified. As already said, the split-off exciton levels are resonant states because they can decay into the continuum of the main exciton series. The intrinsic half-width $\Gamma(1s)$ of the ground state is also given in Tables III and IV. These values cannot be directly compared with experiment and cannot be used to establish if the split-off exciton states can be experimentally observed, because other decay mechanisms are generally present (such as phonon or impurity scattering) which can additionally broaden the exciton peaks appreciably.[64]

The agreement of our results with experiment is generally satisfactory and could be improved when more accurate band parameters will be available. The only case in which there is a large discrepancy between theoretical and experimental results is GaP. Because for this compound the coupling parameter Φ has a small value, our method is certainly applicable, and therefore the above disagreement must be attributed to the values of the parameters used in the calculation, supposing that

TABLE III. Results for Ge and III-V compounds. All the quantities are defined in the text. The last column gives the reference for the valence-band parameters used in the calculation. The blanks mean lacking experimental results and the dots indicate a number smaller than 10^{-2} meV. The energy unit is meV.

	R_0	E_d	E_{so}	$E_b(1s, \Gamma_8)$ Theor	$E_b(1s, \Gamma_8)$ Expt	$E_b(2s, \Gamma_8)$	$E_b(1s, \Gamma_6)$	$\Gamma(1s)$	Ref.
AlAb	1.44	...	...	1.44		0.36	1.44	...	17
	1.45	...	...	1.45		0.36	1.45	...	43
GaP	8.30	0.11	0.03	8.44	3.5 (Ref. 59)	2.13	8.23	0.15	17
	8.91	0.45	0.11	9.47		2.43	8.64	0.66	43
GaAs	4.16	0.10	...	4.26		1.08	4.14	0.01	17
	4.22	0.18	...	4.40	4.4 (Ref. 61)	1.13	4.19	0.02	43
	3.90	0.18	...	4.08		1.04	3.87	0.01	60
GaSb	2.05	0.06	...	2.11		0.54	2.05	0.01	17
	1.87	0.13	...	2.00		0.52	1.87	0.01	43
	1.82	0.09	...	1.91		0.49	1.82	0.01	47
InP	4.96	0.17	0.01	5.14	4.0 (Ref. 62)	1.31	4.93	0.03	17
	4.82	0.33	0.02	5.17		1.34	4.75	0.06	43
InAs	1.74	0.09	...	1.83		0.47	1.74	...	17
	1.68	0.10	...	1.78		0.46	1.68	...	43
	1.57	0.12	...	1.69		0.44	1.57	...	40
InSb	0.56	0.02	...	0.58		0.15	0.56	...	17
	0.49	0.04	...	0.53	~0.4 (Ref. 5)	0.14	0.49	...	43
	0.48	0.04	...	0.52		0.14	0.48	...	48
Ge	1.49	0.08	...	1.57	~1.6 (Ref. 63)	0.40	1.49	...	43
	1.44	0.09	...	1.53		0.40	1.44	...	49

TABLE IV. Results for cubic II-VI compounds. The energy unit and the symbols are those used in Table III.

	R_0	E_d	E_{so}	$E_b(1s, \Gamma_8)$ Theor	$E_b(1s, \Gamma_8)$ Expt	$E_b(2s, \Gamma_8)$	$E_b(1s, \Gamma_6)$	$\Gamma(1s)$	Ref.
ZnS	36.87	0.75	0.40	38.02		9.61	37.59	5.06	17
	47.41	6.38	3.69	57.48		15.29	60.01	45.51	43
ZnSe	22.43	0.38	0.06	22.87	21.0 (Ref. 36)	5.77	22.28	0.25	17
	23.67	2.44	0.40	26.51		6.95	22.65	1.70	43
ZTe	9.26	0.05	. . .	9.31	10.0 (Ref. 45)	2.34	9.25	. . .	17
	10.83	0.36	0.02	11.21		2.85	10.79	0.03	43
CdTe	11.43	0.15	. . .	11.58	10.0 (Ref. 4)	2.92	11.41	0.01	17
	10.10	0.58	0.03	10.71		2.76	10.03	0.04	43

the experimental estimate of the binding energy is correct.

It is interesting to discuss the sensitivity of the results with respect to the choice of the parameters used. The quantity which has to be accurately determined is the effective Rydberg, and this means that the dielectric constant ϵ_0, the electron effective mass m_e^*, and the Luttinger valence-band parameter γ_1 require high accuracy. The results are generally less sensitive to the other valence parameters.

The binding energy of the split-off exciton given in Table III has been obtained assuming the same effective mass for both valence bands. As already noted, the split-off band should have a different mass for compounds like GaSb, InAs, and InSb where the spin-orbit splitting is comparable or even larger than the energy gap. Reduced effective masses of the split-off exciton are available for GaSb[12] and InAs,[14] where experiments give for μ_0 the values $0.034m_0$ and $0.020m_0$, respectively. Using these values, the binding energy of the split-off series is 1.98 and 2.00 meV for GaSb and InAs, respectively.

Before concluding, it is worth emphasizing that the present method allows a complete description of the effect of the split-off valence states on the exciton energy levels. The case of an ideal semiconductor with $\Phi = 0.5$ is shown in Fig. 4. As one can see, such effect can increase the binding energies by about 10% at most. This correction is much smaller than what is usually expected. The reason for this is that, even though the split-off contribution increases as $\Delta \to 0$, its magnitude is scaled by the coupling parameter Φ as shown in expressions (13a) and (13b).

IV. CONCLUSIONS

We have shown that direct-exciton spectra in diamond and zinc-blende crystals can be easily investigated in spite of the degeneracy of the valence band. Using symmetry considerations, we have shown that the complications arising from the valence bands can be overcome, and a method comparable for simplicity to that for simple bands is obtained.

Our results show that the previously used simple model in which the degenerate valence bands are replaced by an "average" simple band can be satisfactory and, in addition, they show how the mass of this "average" simple band is related to actual valence-band parameters. The accuracy of this simple model has been obtained from the evaluation of the most important corrections to it. Their magnitude depends on a coupling parameter Φ which is simply connected to the band parameters. As a consequence of these corrections, the Rydberg law is no longer satisfied. The effects of inversion asymmetry are shown to be extremely small and very difficult to be experimentally observed. In the present treatment, we have neglected effects due to the exchange interaction because they are generally difficult to observe. However, our method can be easily extended to include such effects.

This method has the same accuracy as the previously used variational method for the ground state of the main series, but it is better in two respects:

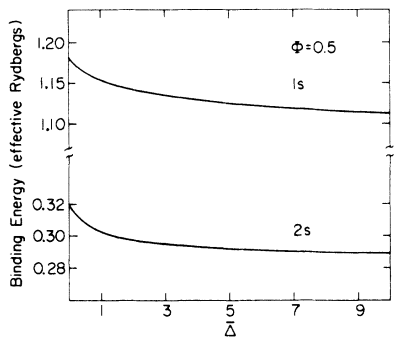

FIG. 4. Binding energy for the 1s and 2s main exciton states versus the spin-orbit splitting $\bar{\Delta}$ for an ideal semiconductor with a coupling parameter $\Phi = 0.5$. All energies are in units of the effective Rydberg.

its simplicity and the fact that it allows also the investigation of excited states of the main series and the split-off series.

It is to be mentioned that our method cannot be applied, as it is, to the problem of acceptor states because in these cases the coupling parameter Φ can be so large that perturbation theory is not valid. However, our method can be extended to any number of degenerate bands and any kind of crystal symmetry as long as terms of lower symmetry in the exciton Hamiltonian can be treated by perturbation theory. Indirect excitons in group-IV elements and III-V compounds can be investigated with the same method, because in these cases the coupling parameter Φ is sufficiently small. Finally, one can also study the effects of weak external fields or small strains on the exciton energy levels. These problems are presently under investigation.

APPENDIX

In this Appendix we drive expressions (13a)–(13d) and (22) starting from (12a)–(12d) and (21), respectively. We first consider expression (12a) and we write it in the following condensed form:

$$\Delta E_d(1s) = \mathbf{S}_n \sum_{l,m} \sum_{i=1}^{6} \frac{|\langle n,l,m,i|H_d|1,0,0,1\rangle|^2}{-1-E_{n,i}}, \tag{A1}$$

where the first symbol on the right-hand side means summation over n and integration in k. Performing the summation over i, we get

$$\Delta E_d(1s) = \mathbf{S}_n \sum_{l,m} \left\{ \frac{|\langle n,l,m|\bar{Q}|1,0,0\rangle|^2}{1/n^2-1} + \frac{|\langle n,l,m|\bar{L}^+|1,0,0\rangle|^2}{1/n^2-1} + \frac{|\langle n,l,m|\bar{M}^+|1,0,0\rangle|^2}{1/n^2-1} + \frac{|\langle n,l,m|-(i/\sqrt{2})\bar{L}^+|1,0,0\rangle|^2}{1/n^2-1-\bar{\Delta}} + \frac{|\langle n,l,m|i\sqrt{2}\bar{M}^+|1,0,0\rangle|^2}{1/n^2-1-\bar{\Delta}} \right\}, \tag{A2}$$

where the state $|n,l,m\rangle$ is defined in the text by expression (9) and the operators $\bar{Q}$, $\bar{L}$, and $\bar{M}$ are the dimensionless expressions of the operators Q, L, and M according to the units (7) and (8). The effect of these operators on the ground-state wave function $|1,0,0\rangle$ is

$$\bar{Q}|1,0,0\rangle = -\frac{4}{\sqrt{5}}\frac{\mu_0}{\mu_1}\left[\left(1+\frac{1}{r}\right)e^{-r}\right]Y_2^0, \tag{A3}$$

$$\bar{L}|1,0,0\rangle = -i\frac{2\sqrt{2}}{\sqrt{15}}\frac{\mu_0}{\mu_2}\left[\left(1+\frac{1}{r}\right)e^{-r}\right]Y_2^{-1}, \tag{A4}$$

$$\bar{M}|1,0,0\rangle = \left[\left(\frac{2\sqrt{2}}{\sqrt{5}}\frac{\mu_0}{\mu_1} - (\sqrt{\tfrac{2}{15}})\frac{\mu_0}{\mu_2}\right)Y_2^2 + \left(\frac{2\sqrt{2}}{\sqrt{5}}\frac{\mu_0}{\mu_1} + (\sqrt{\tfrac{2}{15}})\frac{\mu_0}{\mu_2}\right)Y_2^{-2}\right]\left[\left(1+\frac{1}{r}\right)e^{-r}\right], \tag{A5}$$

where Y_l^m are the spherical harmonics.[25] We insert the above expressions into (A2) and perform the summation over l and m. Using the orthogonality relations of the spherical harmonics, we obtain

$$\Delta E_d(1s) = -\tfrac{4}{5}\Phi(\mu_0,\mu_1,\mu_2)\left\{\sum_{n=3}^{\infty}\frac{|I_n|^2}{1-1/n^2}+\int_0^{\infty}dk\,\frac{|I_k|^2}{1+k^2} + \sum_{n=3}^{\infty}\frac{|I_n|^2}{\bar{\Delta}+1-1/n^2}+\int_0^{\infty}dk\,\frac{|I_k|^2}{\bar{\Delta}+1+k^2}\right\}, \tag{A6}$$

where Φ is defined by (14) and

$$I_n = \int_0^{\infty} R_{n2}(r)\,(r+r^2)\,e^{-r}\,dr, \tag{A7}$$

where $R_{nl}(r)$ are the normalized hydrogenic radial wave functions. I_k is defined by expression (A7) after replacing the lower index n by k. Introducing the function $S_1(x)$ defined as

$$S_1(x) = \sum_{n=3}^{\infty}\frac{|I_n|^2}{x+1-1/n^2}+\int_0^{\infty}\frac{|I_k|^2}{x+1+k^2}\,dk, \tag{A8}$$

we obtain

$$\Delta E_d(1s) = -\tfrac{4}{5}\Phi(\mu_0,\mu_1,\mu_2)\,[S_1(0)+S_1(\bar{\Delta})], \tag{A9}$$

which is the expression given in the text.

Following the procedure described above, expressions (13b)–(13d) and (22) are easily obtained from (12b)–(12d) and (21), when the functions $S_2(x)$ and $S_3(x)$ are defined as follows:

$$S_2(x) = \sum_{n=3}^{\infty}\frac{|J_n|^2}{x+\frac{1}{4}-1/n^2}+\int_0^{\infty}dk\,\frac{|J_k|^2}{x+\frac{1}{4}+k^2}, \tag{A10}$$

$$S_3(x) = \sum_{n=2}^{\infty}\frac{|K_n|^2}{x+1-1/n^2}+\int_0^{\infty}dk\,\frac{|K_k|^2}{x+1+k^2}, \tag{A11}$$

and

$$T_1(x) = S_1(-x), \tag{A12}$$

$$T_2(x) = S_2(-x). \tag{A13}$$

The quantities J_n and K_n which appear in (A10) and (A11) are

$$J_n = \int_0^{\infty} R_{n2}(r)\,(r+\tfrac{1}{2}r^2-\tfrac{1}{8}r^3)\,e^{-r/2}\,dr, \tag{A14}$$

$$K_n = \int_0^\infty R_{n1}(r)\, r^2 e^{-r}\, dr\,. \tag{A15}$$

Analogous expressions define J_k and K_k.

The quantities I_n, J_n, K_n, I_k, J_k, and K_k are defined in terms of integrals involving discrete and continuum hydrogenic radial wave functions. These integrals can be exactly evaluated and, after straightforward but lengthy calculations, can be reduced to the following compact expressions:

$$I_n = \left(\frac{n}{(n^2-1)(n^2-4)}\right)^{1/2} \left[3 - \frac{19n^2+5}{n^2-1}\left(\frac{n-1}{n+1}\right)^n\right], \tag{A16}$$

$$J_n = \left(\frac{n}{(n^2-1)(n^2-4)}\right)^{1/2} \times \left[3 - \frac{135n^4 - 136n^2 - 80}{(n^2-4)^2}\left(\frac{n-2}{n+2}\right)^n\right], \tag{A17}$$

$$K_n = 4\left(\frac{n}{n^2-1}\right)^{3/2}\left(\frac{n-1}{n+1}\right)^n, \tag{A18}$$

$$I_k = \left\{\frac{k}{[1-e^{-2\pi/k}](1+k^2)(1+4k^2)}\right\}^{1/2} \times \left[3 + \frac{5k^2-19}{k^2+1}\, e^{-2\arctan(k)/k}\right], \tag{A19}$$

$$J_k = \left\{\frac{k}{[1-e^{-2\pi/k}](1+k^2)(1+4k^2)}\right\}^{1/2} \times \left[3 + \frac{80k^4 - 136k^2 - 135}{(1+4k^2)^2}\, e^{-2\arctan(2k)/k}\right], \tag{A20}$$

$$K_k = 4\left\{\frac{k}{[1-e^{-2\pi/k}](1+k^2)^3}\right\}^{1/2} e^{-2\arctan(k)/k}. \tag{A21}$$

Using the above expressions, the functions (A8) and (A10)–(A13) can be computed to any degree of accuracy (we have computed them to six decimal figures).

The same procedure can be used to obtain expressions (16a) and (16b) from (15a) and (15b). In this case the functions $\gamma_1(x)$ and $\gamma_2(x)$ are defined as follows:

$$\gamma_1(x) = \tfrac{8}{5}\pi\,|I_k|^2/k \quad \text{with } k = (x-1)^{1/2}\,, \tag{A22}$$

$$\gamma_2(x) = \tfrac{1}{5}\pi\,|J_k|^2/k \quad \text{with } k = (x-\tfrac{1}{4})^{1/2}\,. \tag{A23}$$

In a previous paper[18] we have used the values $\frac{25}{112}$ and $\frac{3}{16}$ for $S_1(0)$ and $S_3(0)$, respectively. The value $S_3(0) = \frac{3}{16}$ was obtained considering the following fictitious Hamiltonian:

$$H_1 = p^2/2m - e^2/r + \alpha p_z\,. \tag{A24}$$

The ground-state energy of (A24) can be obtained exactly with a translation of the momentum p_z and is

$$E_{10} = -me^4/2\hbar^2 - \tfrac{1}{2}\alpha^2 m\,. \tag{A25}$$

The same energy to second order in α can be obtained considering the last term in (A24) as a perturbation. The result is

$$E'_{10} = -me^4/2\hbar^2 - \tfrac{8}{3}\alpha^2 m S_3(0)\,. \tag{A26}$$

Comparing (A25) and (A26), we get the exact value

$$S_3(0) = \tfrac{3}{16}\,.$$

By numerically computing $S_3(0)$ as given by (A11) we get the value 0.187 500. The value $S_1(0) = \frac{25}{112}$ can be obtained using the same technique and introducing the fictitious Hamiltonian

$$H_2 = \frac{p^2}{2m} - \frac{e^2}{r} + \frac{\beta}{2m}\,(p_x^2 + p_y^2 - 2p_z^2)\,. \tag{A27}$$

The ground-state energy of (A27) cannot be obtained exactly and we have evaluated it using the variational method. Following Kohn and Luttinger,[65] we use the ground-state trial function

$$\Psi = (\pi a^2 b)^{-1/2} \exp\left[-\left(\frac{x^2+y^2}{a^2} + \frac{z^2}{b^2}\right)^{1/2}\right]. \tag{A28}$$

After lengthy calculations, we obtain the approximate ground-state energy to second order in β,

$$E_{20} = -(me^4/2\hbar^2)\,[1 + \tfrac{5}{7}\beta^2]\,. \tag{A29}$$

The exact ground-state energy to second order in β can be obtained considering the last term in (A27) as a perturbation. The result is

$$E'_{20} = -(me^4/2\hbar^2)\,[1 + \tfrac{16}{5}\beta^2 S_1(0)]\,. \tag{A30}$$

Comparing (A29) and (A30), we get

$$S_1(0) \cong \tfrac{25}{112} = 0.223\,214\,.$$

By numerically computing $S_1(0)$ using expression (A8), we get $S_1(0) = 0.224\,632$, which slightly improves the previous value.

---

*Research supported in part by the Advanced Research Projects Agency under Contract No. HC-15-67-C-0221 and in part by the U.S. Air Force Office of Scientific Research under Contract No. AF-AFOSR-328-67.

[1]G. G. Macfarlane, T. P. MeLean, J. E. Quarrington, and V. Roberts, Phys. Rev. 108, 1377 (1957); 111, 1245 (1958); J. Phys. Chem. Solids 8, 388 (1959); Proc. Phys. Soc. (London) 71, 863 (1958); S. Zwerdling, L. M. Roth, and B. Lax, Phys. Rev. 109, 2207 (1958); J. Phys. Chem. Solids 8, 397 (1959).

[2]E. J. Johnson, in *Semiconductors and Semimetals*, edited by K. Willardson and A. Beer (Academic, New York, 1967), Vol. 3, p. 153; J. Phys. Chem. Solids 8, (1959).
[3]B. Segall and D. T. F. Marple, in *Physics and Chemistry of II-VI Compounds*, edited by M. Aven and J. Prener (North-Holland, Amsterdam, 1967), p. 317.
[4]E. J. Johnson, Phys. Rev. Letters 19, 352 (1967).
[5]G. H. Wannier, Phys. Rev. 52, 191 (1937). For a general review of exciton theory see R. S. Knox, in *Solid State Physics*, edited by F. Seitz and D. Turnbull (Academic, New York, 1963), Suppl. 5.
[6]R. J. Elliott, Phys. Rev. 108, 1384 (1957).
[7]J. Dresselhaus, J. Phys. Chem. Solids 1, 14 (1956).
[8]J. M. Luttinger and W. Kohn, Phys. Rev. 97, 869 (1955).
[9]T. P. McLean and R. Loudon, J. Phys. Chem. Solids 13, 1 (1960).
[10]W. Kohn and D. Schechter, Phys. Rev. 99, 1903 (1955).
[11]Y. Abe, J. Phys. Soc. Japan 19, 818 (1964).
[12]M. Reine, R. L. Aggarwal, and B. Lax, Solid State Commun. 8, 35 (1970).
[13]B. O. Seraphin and R. B. Hess, Phys. Rev. Letters 14, 138 (1965).
[14]C. R. Pidgeon, S. H. Groves, and J. Feinleib, Solid State Commun. 5, 677 (1967).
[15]M. Aven, D. T. F. Marple, and B. Segall, J. Appl. Phys. Suppl. 32, 2261 (1961); A. C. Aten, C. Z. Van Doorn, and A. T. Vink, in *Proceedings of the International Conference of the Physics of Semiconductors, Exeter* , edited by A. C. Strickland (The Institute of Physics and the Physical Society, London, 1962), p. 696.
[16]M. A. Gilleo, P. T. Bailey, and D. E. Hill, Phys. Rev. 174, 898 (1968).
[17]R. L. Bowers and G. D. Mahan, Phys. Rev. 185, 1073 (1969), and cited references.
[18]A. Baldereschi and N. O. Lipari, Phys. Rev. Letters 25, 373 (1970).
[19]M. L. Cohen and T. K. Bergstresser, Phys. Rev. 141, 789 (1966); F. H. Pollak, C. W. Higginbotham, and M. Cardona, J. Phys. Soc. Japan Suppl. 21, 20 (1966). See also the review articles by F. G. Bassani, in *Semiconductors and Semimetals*, edited by K. Willardson and A. Beer (Academic, New York, 1966), Vol. 1, p. 21; and by B. Segall, in *Physics and Chemistry of II-VI Compounds*, edited by M. Aven and J. Prener (North-Holland, Amsterdam, 1967), p. 1.
[20]R. H. Paramenter, Phys. Rev. 100, 573 (1955); G. Dresselhaus, *ibid.* 100, 580 (1955); E. O. Kane, J. Phys. Chem. Solids 1, 249 (1957).
[21]M. L. A. Robinson, Phys. Rev. Letters 17, 963 (1966); D. G. Seiler and W. M. Becker, Phys. Letters 26A, 96 (1967); C. R. Pidgeon and S. H. Groves, Phys. Rev. Letters 20, 1003 (1968); M. A. Gilleo and P. T. Bailey, Phys. Rev. 187, 1181 (1969).
[22]J. M. Luttinger and W. Kohn, Phys. Rev. 97, 869 (1955).
[23]J. M. Luttinger, Phys. Rev. 102, 1030 (1956).
[24]G. Dresselhaus, A. F. Kip, and C. Kittel, Phys. Rev. 98, 368 (1955).
[25]L. D. Laundau and E. M. Lifshitz, *Quantum Mechanics* (Pergamon, Oxford, 1965), Chap. 5.
[26]V. Weisskopf and E. Wigner, Z. Physik 63, 54 (1930); 65, 18 (1930).
[27]G. Dresselhaus and M. S. Dresselhaus, in *The Optical Properties of Solids*, edited by J. Tauc (Academic, New York, 1966), p 198.
[28]W. J. Turner and W. E. Reese, Phys. Rev. 127, 126 (1962).
[29]P. J. Dean, C. H. Henry, and C. J. Frosch, Phys. Rev. 168, 812 (1968).
[30]K. G. Hambleton, C. Hilsum, and B. R. Holeman, Proc. Phys. Soc. (London) 77, 1147 (1961).
[31]G. Picus, E. Burstein, and B. H. Henvis, J. Phys. Chem. Solids 8, 282 (1959).
[32]W. J. Turner, W. E. Reese, and G. D. Pettit, Phys. Rev. 136, A1467 (1964).
[33]O. G. Lorimor and W. G. Spitzer, J. Appl. Phys. 36, 1841 (1965).
[34]R. A. Faulkner, Phys. Rev. 184, 713 (1969).
[35]D. Berlincourt, H. Jaffe, and R. L. Shiozawa, Phys. Rev. 129, 1009 (1963).
[36]G. E. Hite, D. F. T. Marple, M. Aven, and B. Segall, Phys. Rev. 156, 850 (1967).
[37]R. Kaplan, M. A. Kinch, and W. C. Scott, Solid State Commun. 7, 883 (1969); G. E. Stillman, C. M. Wolfe, and J. O. Dimmock, *ibid.* 7, 921 (1969).
[38]R. Braunstein and E. O. Kane, J. Phys. Chem. Solids 23, 1423 (1962).
[39]Y. A. Makhalov and R. L. Melik-Davtyan, Fiz. Tverd. Tela 11, 2667 (1969) [Soviet Phys. Solid State 11, 2155 (1970)].
[40]C. R. Pidgeon, D. L. Mitchell, and R. N. Brown, Phys. Rev. 154, 737 (1967).
[41]C. R. Pidgeon and R. N. Brown, Phys. Rev. 146, 575 (1966).
[42]R. L. Aggarwal, Phys. Rev. B 2, 458 (1970).
[43]M. Cardona, J. Phys. Chem. Solids 24, 1543 (1963).
[44]D. T. F. Marple, J. Appl. Phys. 35, 1879 (1964).
[45]R. E. Nahory and H. Y. Fan, Phys. Rev. Letters 17, 251 (1966).
[46]K. K. Kanazawa and F. C. Brown, Phys. Rev. 135, A1757 (1964).
[47]R. A. Straddling, Phys. Letters 20, 217 (1966).
[48]C. R. Pidgeon and S. H. Groves, Phys. Rev. 186, 824 (1969).
[49]J. C. Hensel and K. Suzuki (unpublished).
[50]M. Cardona (unpublished results cited in Bowers and Mahan, Ref. 17).
[51]M. Cardona, F. H. Pollak, and K. L. Shaklee, Phys. Rev. Letters 16, 644 (1966).
[52]M. Cardona, K. L. Shaklee, and F. H. Pollak, Phys. Rev. 154, 696 (1967).
[53]S. A. Abagyan and V. K. Subashev, Fiz. Tverd. Tela 6, 3168 (1964) [Soviet Phys. Solid State 6, 2529 (1965)].
[54]S. Zwerdling, B. Lax, K. J. Button, and L. M. Roth, J. Phys. Chem. Solids 9, 320 (1959).
[55]E. D. Palik and J. R. Stevenson, Phys. Rev. 130, 1344 (1963).
[56]M. Rouzeyre, H. Mathieu, D. Auvergne, and J. Camassel, Solid State Commun. 7, 1219 (1969).
[57]Cohen and Bergstresser, Ref. 19.
[58]M. D. Sturge, Phys. Rev. 127, 768 (1962).
[59]V. K. Subashiev and G. A. Chalikyan, Fiz. Tverd. Tela 7, 1237 (1965) [Soviet Phys. Solid State 7, 992 (1965)].
[60]Q. H. F. Vrehen, J. Phys. Chem. Solids 29, 129 (1968).
[61]M. A. Gilleo, P. T. Bailey, and D. E. Hill, J. Luminescence 1/2, 562 (1970).
[62]U. Heim, O. Roder, and M. H. Pilkuhn, Solid State Commun. 7, 1173 (1969).

[63]E. J. Johnson, in *Proceedings of the Ninth International Conference on the Physics of Semiconductors, Moscow*, 1968 (Nauka, Leningrad, 1968), p. 276.

[64]P. Lawaetz and D. D. Sell (unpublished).

[65]W. Kohn and J. M. Luttinger, Phys. Rev. 98, 915 (1955).

PHYSICAL REVIEW B VOLUME 3, NUMBER 2 15 JANUARY 1971

Extension of the Quasicubic Model to Ternary Chalcopyrite Crystals

J. E. Rowe
Bell Telephone Laboratories, Murray Hill, New Jersey 07974
and
J. L. Shay
Bell Telephone Laboratories, Holmdel, New Jersey 07733
(Received 19 June 1970)

A simple theoretical model is proposed to explain the recently observed valence-band structure of $CdSnP_2$ and similar chalcopyrite crystals. The valence bands of a chalcopyrite crystal are regarded as equivalent to those of a strained version of its binary analog. This model predicts the signs and magnitudes of the valence-band splittings observed in $CdSnP_2$ and $ZnSiAs_2$. We show further that the quasicubic model explains quantitatively the unusual polarization dependences previously reported.

It has recently been reported[1] that the polarization selection rules governing the band-edge electroreflectance and photoreflectance spectra of $CdSnP_2$ are opposite to those observed in wurtzite II-VI semiconductors and to theoretical predictions for similar chalcopyrite semiconductors. To explain this result, a new valence-band model was proposed[1] with the essential feature that the sign of the crystal-field splitting was opposite to that observed in wurtzite II-VI semiconductors. It is the purpose of this paper to provide a theoretical explanation for the proposed valence-band model, based on a very simple approximation to the crystal potential in chalcopyrite crystals. We show that the signs and magnitudes of the valence-band splittings in $CdSnP_2$ and $ZnSiAs_2$ (the only crystals for which electroreflectance data are available) can be predicted from the known properties of the binary analogs of these materials (e.g., InP is the binary analog of $CdSnP_2$). We further show that the quasicubic model, developed by Hopfield[2] to explain properties of wurtzite crystals, can also be applied to chalcopyrite crystals with the result that the unusual polarization dependences observed experimentally can be explained quantitatively.

The valence-band model previously proposed[1] to explain the electroreflectance and photoreflectance spectra of $CdSnP_2$ is shown in Fig. 1. The triply degenerate Γ_{15} in zinc blende is split in chalcopyrite such that the nondegenerate level Γ_4 lies above the doubly degenerate Γ_5, just opposite to the ordering observed in wurtzite semiconductors. The doubly degenerate state is then split by the spin-orbit interaction. Hopfield's[2] quasicubic model regards the wurtzite crystal-field splitting as equivalent to the splitting produced by a trigonal uniaxial stress applied to a zinc-blende crystal. The strain

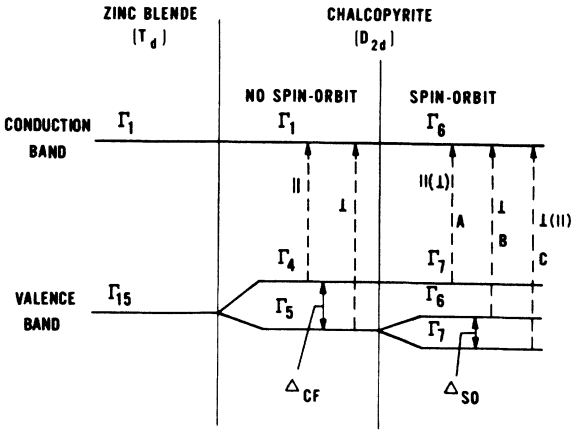

FIG. 1. Band structure and selection rules at $k = [000]$ in zinc blende and chalcopyrite for light polarized relative to the optic axis. A, B, and C refer to the three peaks observed in electroreflectance spectra (Refs. 1 and 6). For the polarizations shown in parentheses, the transitions are allowed group theoretically but will be observed only to the extent that spin-orbit coupling mixes the unperturbed wave functions. For a finite Δ_{cf} and Δ_{so}, the valence-band splittings must be determined using Eq. (1). For example, the separation of the Γ_7 and Γ_6 levels will be equal to Δ_{so} only in the limit that $\Delta_{so} \gg \Delta_{cf}$ and will be equal to $(\frac{2}{3})\,\Delta_{so}$ in the limit that $\Delta_{so} \ll \Delta_{cf}$.